

Article

Surface Imprinted Layer of Cypermethrin upon Au Nanoparticle as a Specific and Selective Coating for the Detection of Template Pesticide Molecules

Jaya Sitjar ¹, Ying-Chen Hou ¹, Jiunn-Der Liao ^{1,2,*}, Han Lee ¹, Hong-Zheng Xu ¹, Wei-En Fu ³ and Guo Dung Chen ³

¹ Department of Materials Science and Engineering, National Cheng Kung University, 1 University Road, Tainan 701, Taiwan; jaya.sitjar@gmail.com (J.S.); k03200728@gmail.com (Y.-C.H.); rick594007@hotmail.com (H.L.); az436436@gmail.com (H.-Z.X.)

² Medical Device Innovation Center, National Cheng Kung University, 1 University Road, Tainan 701, Taiwan

³ Center for Measurement Standards, Industrial Technology Research Institute, No. 321, Kuang Fu Road, Sec. 2, Hsinchu 300, Taiwan; weienfu@itri.org.tw (W.-E.F.); eric_chen@itri.org.tw (G.D.C.)

* Correspondence: jdliao@mail.ncku.edu.tw; Tel.: +886-6-2757575 (ext. 62971); Fax: +886-6-2346290

Received: 30 June 2020; Accepted: 30 July 2020; Published: 1 August 2020



Abstract: The detection of specific pesticides on food products is essential as these substances pose health risks due to their toxicity. The use of surface-enhanced Raman spectroscopy (SERS) takes advantage of the straightforward technique to obtain fingerprint spectra of target analytes. In this study, SERS-active substrates are made using Au nanoparticles (NPs) coated with a layer of polymer and followed by imprinting with a pesticide–Cypermethrin, as a molecularly imprinted polymer (MIP). Cypermethrin was eventually removed and formed as template cavities, then denoted as Au NP/MIP, to capture the analogous molecules. The captured molecules situated in-between the areas of high electromagnetic field formed by plasmonic Au NPs result in an effect of SERS. The formation of Au NP/MIP was, respectively, studied through morphological analysis using transmission electron microscopy (TEM) and compositional analysis using X-ray photoelectron spectroscopy (XPS). Two relatively similar pesticides, Cypermethrin and Permethrin, were used as analytes. The results showed that Au NP/MIP was competent to detect both similar molecules despite the imprint being made only by Cypermethrin. Nevertheless, Au NP/MIP has a limited number of imprinted cavities that result in sensing only low concentrations of a pesticide solution. Au NP/MIP is thus a specific design for detecting analogous molecules similar to its template structure.

Keywords: surface-enhanced Raman spectroscopy; gold nanoparticles; molecularly imprinted polymer; Cypermethrin; Permethrin

1. Introduction

Techniques to detect chemicals in food, biological, and environmental samples are continuously being studied as there is a need for rapid and accurate methods to efficiently perform analyte detection under urgent cases. [1,2] The main drawback of conventional methods such as chromatography and mass spectroscopy is the long processing times due to the involvement of sample collection and preparation, which most often require multiple steps, even destroying the samples if needed as a result of combustion and/or ionization. [3,4] Nondestructive detection methods such as surface-enhanced Raman spectroscopy (SERS) has been a topic of interest through minimal to no sample preparation in addition to its fast analyte detection capability [5]. Most importantly, it could even detect analytes at trace levels of concentration [6].

The enhancement of Raman-active signals in a target species through the SERS technique is quite based on the use of a SERS-active substrate, which is preferably composed of plasmonic nanostructures and usually made by noble metals such as Au and Ag [7,8]. When the custom-made nanostructure is ignited by a Raman laser, the electrons oscillate with the incident light; this phenomenon is referred to as localized surface plasmon resonance (LSPR) [9–11]. This leads to an enhancement of the electric field that is localized around the nanostructures, consequently enhancing the resulting Raman signals [12]. Varying the geometrical properties of nanostructures could tune the resulting LSPR so that signal enhancement could be optimized. Besides this, efficiently capturing analyte molecules within the nanostructures are equally important. [13].

Applications that call for selectivity and specificity in detecting particular analyte/s have utilized antibodies [14] and aptamers [15] that could be functionalized onto the surface of SERS-active substrate [16,17], resulting in sensitive detection with an ability to detect analytes such as pesticides at low concentrations. In fact, a study was able to combine immunochromatographic assay with SERS, utilizing pesticide immunoprobes to selectively capture specific pesticides and was able to demonstrate sensitive detection with good reproducibility [18]. The said study was able to create a strip with the immunoprobes, which would be suitable in applications calling for multiplex detection. Such functional surface is mainly to capture the analytes, or to introduce non-SERS-active components such as particular oxides, which exhibit strong affinities to the target analyte/s [19]. Alternatively, the use of molecularly imprinted polymers (MIP) coupled with SERS-active substrate, commonly referred to as MIP-SERS [20] has shown promising results in specific analyte detection by combining the sensitivity brought by SERS and selectivity through specific molecule recognition ability of MIP [21–23]. Template molecules, which in the case of MIP-SERS are the target analytes, are imprinted on a polymer matrix that is integrated onto surfaces of plasmonic nanostructures [17,24,25]. As a result, template molecules are then removed, leaving behind complementary sites wherein analytes could rebind, triggering a vibrational change in the system. The reintegrated system reflects in the resulting SERS spectra and realizes the characteristic peaks of the target analyte. MIPs basically serve as gates for selected analytes to go through the polymer layer to reach the inner plasmonic core for SERS, and to take an effect [26].

The most common MIP-SERS structure is the core–shell as it maximizes the use of the surface of plasmonic nanostructures where binding sites are distributed on the said surfaces [27,28]. It has also been found that the SERS effects brought by this structure can be tuned by varying the shell thickness so that strong SERS signals could be observed only up to a limit. Beyond this limit, the intensities of peaks tend to be significantly weakened as the analytes get farther away from the plasmonic core [26]. One major advantage of the core–shell structures is the formation of over-irregular structures, especially for those involving bulk MIPs, whereas MIP layers on core–shell structures are evenly coated on the surface of the plasmonic nanostructures, making it easier to extract the template molecules [29,30]. Unlike in the irregular MIPs, the templates are deeply embedded into the crosslinked bulk material that makes it hard to remove. The fabrication process for this type of MIPs is straightforward wherein synthesized colloidal nanoparticles are coated with a layer of polymer together with the template molecules, which are removed after the polymerization process [20,31,32].

To be able to recognize analyte molecules through MIP-SERS substrates, it is important to consider that this selectivity is highly dependent on the spatial configuration. It is important to note that the imprints exhibit a variety of orientations as a result of the varying configurations of the template molecules as they are integrated into the polymer network. Therefore, to obtain intense SERS signals by maximizing the target molecule-capturing ability of the imprint, the captured target molecule should preferably enter the imprint with its exact same orientation [22]. Another instance to be considered is the possibility of the MIP cavities not to maintain their size and shape owing to the swelling of the polymer when it is prepared in solvent [26]. In addition, MIPs are highly crosslinked so their polymer chains could hinder the analytes that try to enter the cavities. On another note, there could be cases wherein some template molecules are still retained on the polymeric matrix even after the removal

process. Small template molecules such as pesticides are also easier to remove compared to larger ones, that is also why the detection of small molecules are more effective when MIP-SERS platform is used.

In this study, core-shell MIP-SERS nanostructures are synthesized to be utilized as a SERS substrate in the selective detection of a common pesticide. The aim is to combine the effect of SERS brought by the core of Au NP with a layer of MIP imprinted with pesticide molecules. This integration is anticipated to create a selective detection wherein only the specific pesticide can be captured by the MIP imprints, bringing the analyte molecules closer to the plasmonic core resulting in enhanced SERS signals. In summary, an illustration of the reaction mechanism will then be proposed.

2. Experimental Section

2.1. Au NP/MIPs Synthesis and Preparation

Au NPs ranging at 12–20 nm in diameter were first synthesized through the citrate reduction method [33]. Diluted gold tetrachloride (HAuCl_4 , 1 wt %, 1.2 mL diluted in 50 mL DI H_2O) was placed in a double-necked flask attached with a glass condenser; it was then brought to a rapid boil under a silicone oil bath. Upon boiling of HAuCl_4 , trisodium citrate ($\text{Na}_3\text{C}_6\text{H}_5\text{O}_7$, 1 wt %, 2.5 mL) was immediately added; after 5–10 min when the solution achieved a deep red color, it was left to cool down at room temperature. The resulting solution was centrifuged to collect Au NPs. The collected Au NPs were functionalized with (3-mercaptopropyl)trimethoxysilane (MPTMS) under constant stirring in a nitrogen-rich environment at 40 °C for 24 h in a two-necked flat-bottom flask. Note that the MPTMS layer is necessary as it provides the sites for grafting the polymer onto Au NP. Centrifugation (9000 rpm) was then carried out to collect the MPTMS-functionalized Au NPs which were then dried under vacuum; the samples are denoted as Au NP-MPTMS. A layer of Cypermethrin-imprinted polymer on Au NP-MPTMS was then formed through the polymerization of methacrylic acid (MAA) with ethylene glycol dimethacrylate (EGDMA) and azobisisobutyronitrile (AIBN) as the functional monomer, crosslinker, and initiator, respectively. In addition, the polymeric precursors were mixed with Cypermethrin template molecules (2.5 mL 0.001 M Cypermethrin, 0.81 μL MAA, 7.51 mL EGDMA, and 0.03 mg AIBN) to fix the template onto the polymeric matrix while polymerization was done in a nitrogen-rich environment at 65 °C for 12 h (a thin polymer layer) and 24 h (a thick polymer layer), respectively. The resulting polymer-coated Au NPs, denoted as Au NP/Polymer, were centrifuged with ethanol to wash away the unreacted reagents during polymerization and were then mixed with methanol and formic acid under a Soxhlet extractor to remove the Cypermethrin template molecules on the polymer layer; the as-formed sample is then referred to as Au NP/MIP. Afterwards, a subsequent process to rebind Cypermethrin and its similar molecule, Permethrin, to Au NP/MIP is denoted as Au NP/MIP (R). In the following sections, Au NP/MIPs represents the collection of Au NP/Polymer (thin or thick) and Au NP/MIP. The fabrication process is shown in Figure 1.

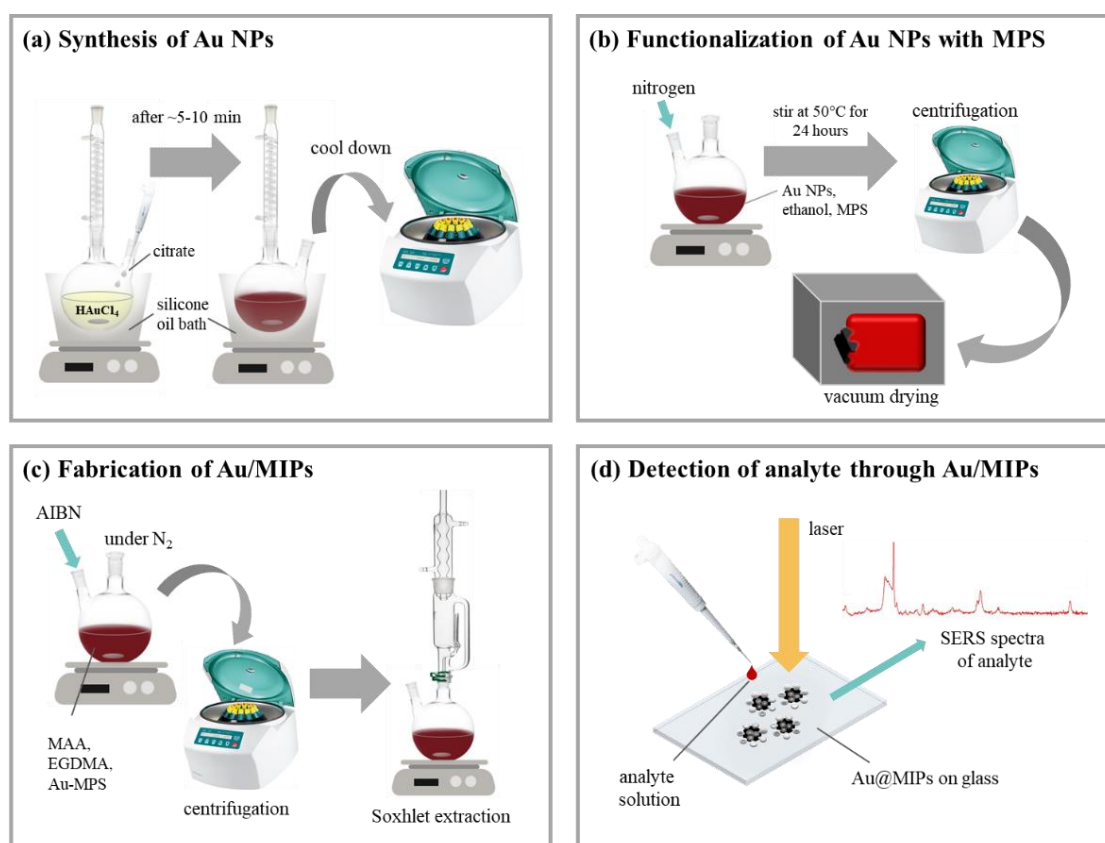


Figure 1. Schematic illustration of the synthesis of Au nanoparticles (NPs)/ molecularly imprinted polymers (MIPs): (a) Synthesis of Au NPs through the reduction of HAuCl₄ by citrate; (b) functionalization of Au NPs by 3-mercaptopropyl)trimethoxysilane (MPTMS) to prepare the surface for polymerization; (c) fabrication of Au NP/MIPs by polymerization on the MPTMS-grafted Au NPs together with the template pesticide molecules which was then followed by their removal through Soxhlet extraction; (d) detection of the analyte solution of pesticide through SERS using the fabricated Au NP/MIPs deposited onto a glass substrate.

2.2. Physical Characterization of Au NP/MIPs

Morphologies of the synthesized Au NP-MPTMS and Au NP/MIPs were analyzed with a high-resolution field-emission scanning electron microscope (FE-SEM, JSM-7000, JEOL, Tokyo, Japan) and transmission electron microscope (TEM, JEM-1400, JEOL, Tokyo, Japan). FE-SEM images were taken using secondary electron imaging mode at an accelerating voltage of 10 kV. The removal degree of template molecule was thereafter estimated by ultraviolet–visible spectroscopy (UV–Vis, U-2010, Hitachi, Tokyo, Japan).

2.3. Compositional Analysis of Au NP/MIPs

X-ray photoelectron spectroscopy (XPS, PHI 5000 VersaProbe, Chigasaki, Japan) was used to determine the presence of elements on Au NP/MIPs as well as to confirm the formation of a thin or thick MIP layer. The resulting XPS spectra were then curve-fitted through Origin 8.0 to identify the elements and functional groups presenting on Au NP/MIPs.

2.4. SERS Property of Au NP/MIPs

Au NP/MIPs and subsequent Au NP/MIP (R) were evaluated for the performance of SERS property using a Raman spectrometer (Renishaw, Wotton-under-Edge, UK). An air-cooled charge-coupled device (CCD) was equipped as a detector with an incident power of 3 mW. Raman measurements were

carried with pesticides: Cypermethrin and Permethrin (Sigma Aldrich; pesticides in powder form, St. Louis, MO, USA) as the target analytes. A fixed amount of these pesticide solutions at varying concentrations (10^{-2} to 10^{-5} M) was dropped onto Au NP/MIPs that were dip-coated upon a clean silicon substrate. The solutions were left to dry on the substrate before acquiring the SERS spectra of the pesticides. The optical microscope of the spectrometer was set at 50 \times magnification and the He-Ne Raman lasers used have a diameter of 1 μ m; the laser excitation wavelengths of 633 and 785 nm with gratings, respectively, at 1800 and 1200 lines/nm were used. Spectrum calibration using a silicon standard was done prior to spectra acquisition.

The resulting SERS spectra were then processed for background removal, baseline correction, and smoothing. Au NP/MIPs were applied to detect trace amounts of pesticides on various types of green tea spiked with the said target analytes. SERS signal collection was performed directly on the as-prepared substrates.

3. Results and Discussion

3.1. Integration of Au NP/MIPs

In Figure 2a, Au NPs before surface modification were well scattered with only a low occurrence of particle agglomeration. In Figure 2b, after MPTMS modification, it appears as though Au NPs agglomerated with the introduction of the MPTMS. Note that MPTMS acts only as an intermediate layer between Au NP core and polymer or MIP shell, its presence on the surface of Au NP is invisible under a microscope. In Figure 2c, the size of Au NPs was estimated by TEM in the range of 12–20 nm, while upon a closer look, an ultra-thin MPTMS layer was observable and estimated around 2.5 nm, as shown in Figure 2d.

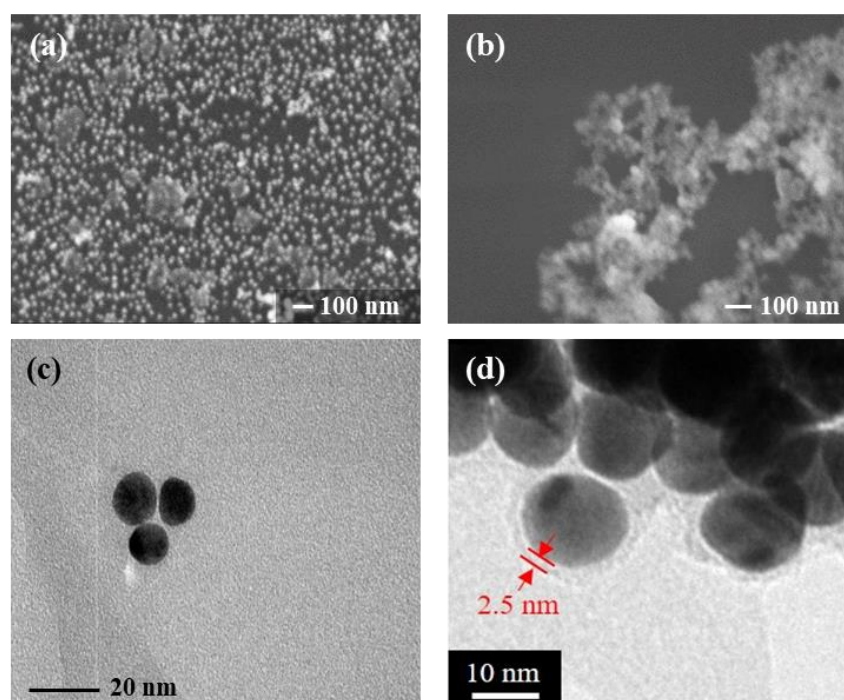


Figure 2. (a) Morphology of the Au NPs before modification with MPTMS appeared to be scattered throughout the substrate while (b) after grafting the MPTMS onto the surface of the Au NPs, the particles became more agglomerated; (c) Au NPs appear to be in a range of 12–20 nm in diameter, with the (d) MTPMS layer with 2.5 nm in thickness.

Agglomeration of Au NP/MIPs is a natural process, which tends to alter the collected quality and quantity of the as-designed particles. To increase the accumulated quantity, Au NP/MIPs would

simultaneously augment surface area available for the subsequent adsorption of rebinding molecules; on the contrary, clustered Au/MIPs might result in reducing the effect of SERS as the imprinted sites for entering the target molecules are presumably restricted by other Au NP/MIPs [33]. Therefore, the study of, e.g., enhancement factor (EF) is relatively unsuitable for interpreting the mechanism of capturing rebinding template molecules.

3.2. Chemical Analyses on the As-Prepared Au NP/MIPs

In Figure 3, the compositions of Au, Au NP-MPTMS, Au NP/Polymer (thin or thick), Au NP/MIP were analyzed step by step along the fabrication process. In Figure 3a, the characteristic binding energy (BE) corresponding to Au 4f (at ~83.0 and ~87.0 eV) was shown. As designed, the intensity of Au NPs drastically decreased with the introduction of MPTMS and completely disappeared as polymer or MIP layer was formed upon MPTMS, regardless of thickness. In Figure 3b, the characteristic BE corresponding to N 1s (at ~399.5 eV) was shown. The presence of N 1s signal is attributed to the N component of Cypermethrin. The N 1s intensities at ~399.5 eV for MIP (Cypermethrin), thin or thick layer were weak owing to very few amounts of the template molecules or subsequent residues remained in the MIP layer.

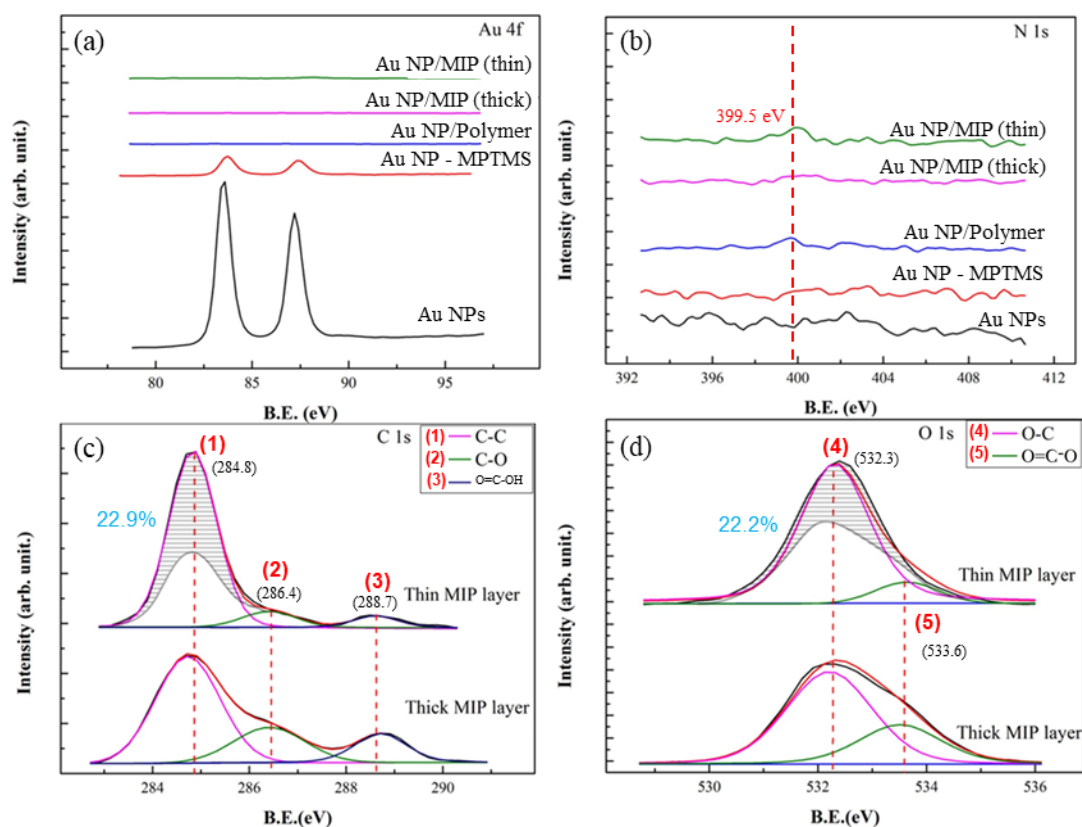


Figure 3. XPS spectra of the Au and Au NP/MIPs to analyze the present elements and groups in each step along the fabrication process. (a) spectra of the substrates corresponding to Au; (b) spectra of the substrates corresponding to N; (c,d) comparisons of the spectra of the Au NP/MIPs with thick and thin layer with respect to functional groups of C and O.

Figure 3c,d, respectively, shows the comparison of resulting C 1s and O 1s spectra of Au NP/MIP with a thin or thick MIP layer. The peaks corresponding to C–O and O=C–OH as exhibited by the Au NP/MIP with a thicker MIP layer are shown to be higher than that of the Au NP/MIP with a thinner MIP layer which on the other hand, exhibits a higher C–C peak. While maintaining the peak ratios of thick MIP (i.e., the peak ratio for 1:2:3 is 4.0:1.5:1.0 and the peak ratio for 4:5 is 2.2:1.0), its spectrum was

superimposed onto the spectrum of the thin one to see the differences in the peak intensities. For the thick MIP layer, the time for polymerization was double than that for the thin one, it is very likely that the residual Cypermethrin molecules and the degree of polymerization may alter the chemical compositions on Au NP/MIP. In Figure 3c,d, taking C 1s and O 1s spectra for the thick MIP layer as the reference, it is assumed that some residual Cypermethrin molecules in the highly polymerized matrix are anticipated. On the other hand, by keeping the same peaks' ratios, less Cypermethrin molecules and more C, O-containing group, shown as the shaded regions of Peaks 1 and 4, in the less polymerized, thin MIP layer resulted.

Furthermore, there could be two factors behind the differences of C 1s and O 1s spectra—chemical and dimensional ones. The chemical factor is much related to the fabrication process of a thin or thick MIP layer, which varies in the required time for polymerization to be completed. To form the thick MIP layer, a longer polymerization time of 24 h was needed, compared to that of 12 h for the thin MIP layer; this gave the MIP to grow longer and thus most of the template Cypermethrin molecules tended to be situated within the polymer matrix instead of the surface, which is the case for the thin MIP. In addition, since the polymerization time for the thin MIP layer is half of that of the thick one, it is most likely that the thin MIP layer would have more unreacted precursors (MAA, EDGMA, AIBN) which are reflected as the differences in the C–C and C–O peak intensities of the thick and thin MIP layers. These factors are anticipated to alter the peaks' intensities at marks 1 and 4 as indicated by the shaded areas.

For the dimensional factor, the chances for Cypermethrin residues to be retained and exposed on the surface of a thin MIP layer are relatively higher as compared with that of a thick MIP layer. In the case of a thick MIP, template molecules are most likely trapped within the polymer and these trapped molecules could not form imprints (i.e., left cavities) on the surface; in the case of a thin MIP layer, more imprints could be formed on the surface.

In summary, a thin-layer Au NP/MIP layer tends to remove the template pesticide molecules easily and to form imprints with a high surface area. Therefore, from XPS C 1s and O 1s spectra, fewer pesticide residues and higher C, O-containing groups attributed to the unreacted polymerization precursors from the thin-layered MIP, as compared to a thick-layered one, can be found. Chemical and dimensional factors as a consequence of the fabrication process are suggested by the resulting Au NP/MIPs.

3.3. Integration of Pesticides into Au NPs/MIPs

It is anticipated that MIPs are imprinted specifically with Cypermethrin molecules, thereafter, only Cypermethrin or molecule/s with an almost similar structure may enter into the imprints of Au NPs/MIPs to be detectable. Both Cypermethrin and Permethrin were used for the verification. Noted that both molecules are classified under the group of pyrethroids, thus they may exhibit almost the same chemical structure.

In Figure 4a,b, the SERS spectra of both pesticides at different concentrations were shown. The peaks at 662, 1002, 1165, 1208, 1615, 1740, and 2253 cm^{-1} corresponding to Cypermethrin, and those to Permethrin were similarly present, except for the peak at 2253 cm^{-1} , which Permethrin does not have. Peak intensities of both pesticides exhibited a similar trend with respect to the analyte concentration. However, as shown in the figure, SERS spectra of Cypermethrin at 10^{-3} M and lower did not show the specific peak at 2253 cm^{-1} , making it similar to the SERS spectra of Permethrin. In this case, the particular use of Au NP/MIPs as a SERS-active substrate is presumably not limited only to the detection of Cypermethrin but also to Permethrin, which makes Au NP/MIPs partially selective to the group of pyrethroids. Moreover, as observed in SERS spectra, the peak intensities of both pesticides at 10^{-4} M and lower exhibited the same as the normal Raman spectra, indicating that Au/MIPs are incapable of detecting ultra-low concentrations of target analytes. In addition, to compare the performance of Au NP/MIPs with bare AuNPs in the detection of pesticides, Figure S1, as shown in the Supplementary Data, demonstrated the SERS spectrum of Cypermethrin at a concentration of 10^{-3} M using bare Au NPs as the substrate; similar peaks were found. The main peak around

1002 cm^{-1} is however sharper for the bare Au NPs than that for Au NP/MIP, most likely because of the presence of the polymer coating in the MIP layer that weakens the electromagnetic fields surrounding Au NP. Despite the bare Au NPs producing a stronger enhancement, the advantage of having a MIP layer coated upon Au NP is that it would only allow specific molecule/s to be detected.

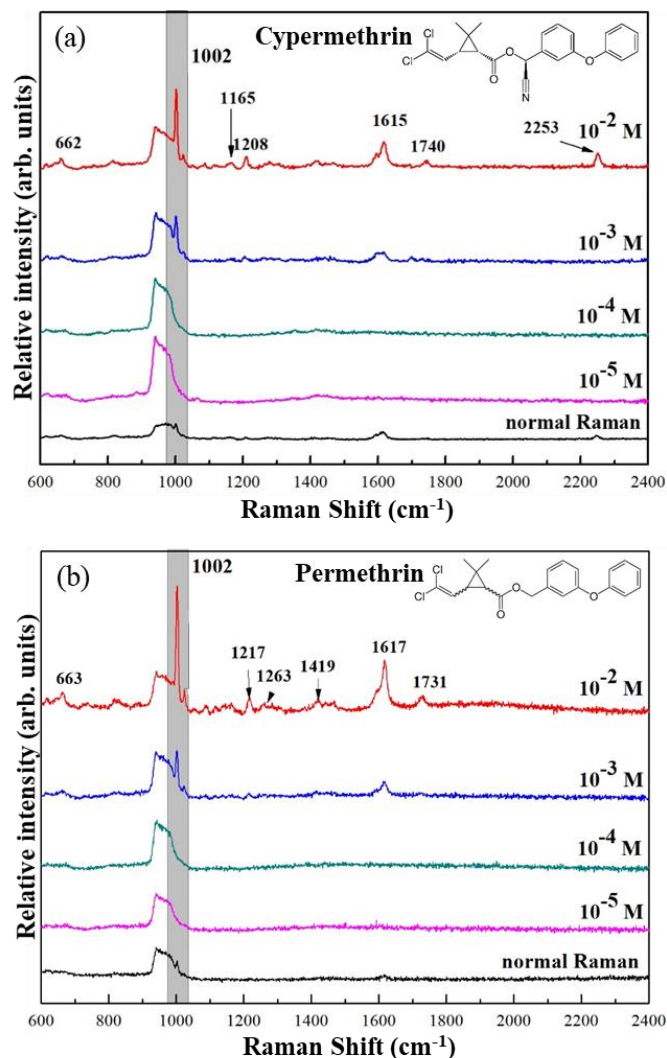


Figure 4. SERS spectra of (a) Cypermethrin and (b) Permethrin at varying concentrations taken with a 633 nm-wavelength laser.

3.4. SERS Mechanisms of Pesticides Detection in Au NPs/MIPs

SERS mechanism of Au NPs/MIPs through two means for detecting both pesticides is proposed. A physical means through electromagnetic mechanism (EM) is driven by the formation of areas of enhancement from overlapping electromagnetic fields surrounding the plasmonic nanostructures as a result of LSPR induced by the incident laser. It is thus dependent on the physical attributes of the nanostructures' shape, size, interstructure distance, among others. However, areas of enhancement are formed only when nanostructures are within a distance of around $\sim 10\text{ nm}$; analyte molecules should then fall within this range for them to be detected effectively to produce SERS signals.

In the case of MIPs, the highest signal enhancement of the analytes would come from those that are captured into the imprints—this way, the analyte molecules are brought closer to the surface of the plasmonic Au NPs and then, the captured analyte is situated in the region between the Au NPs thus the signal enhancing capability of the SERS substrate could be maximized as the analytes are subjected to regions of high electromagnetic fields, which is necessary in the enhancement through

EM, as in the case in the study by Chen and others, wherein analytes enter into the imprint through a “gate effect” [24]. On the other hand, analytes that are not captured inside the imprints are not able to provide signal enhancement as strong as the ones that are captured inside the imprints. For chemical means, although the working principles behind have not been totally understood yet, is based on the modified electronic properties as a result of the formation of a metal–analyte complex. However, the Au NP/MIPs do not exhibit strong affinities to any of the pesticides used in the study and so the chemical enhancement would be almost negligible in the overall enhancement.

Shown in Figure 5, as described in the materials and methods, the Au NPs were subjected to coating with MPTMS first before proceeding to the polymerization to form the MIP layer; template molecules were mixed along with the MIP precursors and in this way, upon the formation of crosslinks within the polymer network, the template molecules would have been immobilized. Template elution was performed to remove the template molecules (outlined shapes), leaving behind imprints on the MIP layer. However, a residual amount of template molecules (solid shapes) still remain on the MIP as Soxhlet extraction is unable to completely remove the template molecules. This would cause errors when used for quantitative applications as the presence of the unremoved template molecules could be interpreted as a false positive—i.e., once the substrate is used for the quantitative detection of the same molecule, results from Raman spectroscopy would recognize both the residual template molecules (solid shapes) and the rebound molecules (dashed shapes) from the sample leading to having a value of the number of molecules detected to be more than the actual value. Thus, there is a need for calibration such that after template elution, the Au NP/MIPs should be subjected to SERS analysis to see if unremoved residual molecules are present on the MIP; if these molecules are present, then it should be taken into account once the substrates are used for further application/s.

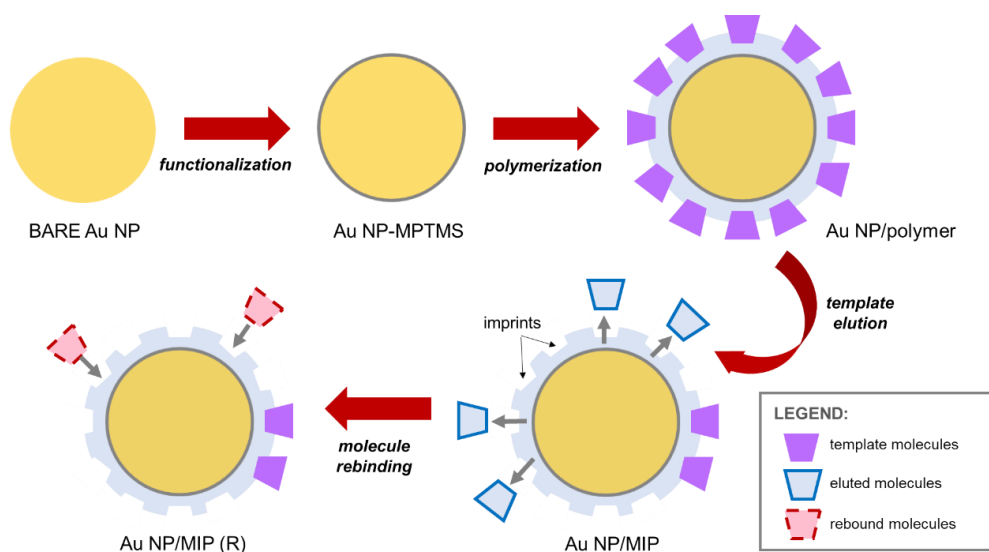


Figure 5. Schematic diagram of the stepwise procedures in the fabrication of Au NP/MIPs—Au NP functionalization with MPTMS followed by polymerization together with template molecules and subsequently, template elution to form molecular imprints wherein rebound molecules would enter during the detection process.

In addition, during analyte detection through the MIP-based system, analyte molecules rebind in the cavities imprinted after template elution; MIPs basically serve as tools to effectively capture the molecules to be detected rather than directly providing a SERS effect. With the involvement of a polymer layer, MIPs often exhibit drawbacks such as unnecessary background signals and noise. Moreover, a study by Wang and others demonstrated that with the increasing thickness of the polymer shell, the contact between the analyte and plasmonic material which is necessary to produce the SERS effect, is retarded, decreasing the charge transfer effect, negatively affecting the resulting SERS

signals [29]. Therefore, in designing a MIP-based system for SERS application, it is important to find an optimal condition to maintain the effect of SERS that generates through a physical means of SERS mechanism even with possible interferences brought by the layer of MIPs.

4. Conclusions

Plasmonic Au nanoparticles were synthesized and combined with the concept of molecular imprinting to create a SERS-active substrate that is able to detect specific target molecule/s. Polymer precursors were mixed with template molecules of Cypermethrin pesticide and polymerization was carried out on the surface of Au NPs. The resulting Au NP/MIPs were able to detect not only Cypermethrin but also Permethrin thus the imprints were able to accommodate molecules with an almost similar structure to the template. The areas of strong electromagnetic fields are located in-between the cavities created by the template molecule imprints as this is where the surfaces of the Au NPs are exposed while electromagnetic fields that are formed in areas aside from the cavity–cavity area are weaker. The probability of having a precise cavity–cavity-formed area of high electromagnetic field enhancement is low thus the Au NP/MIPs are not capable of detecting analytes at low concentrations ($<10^{-4}$). Moreover, it was demonstrated that regardless of the thickness of the MIP layer on Au NP/MIPs, there would somehow be drawbacks—a thin MIP layer would most likely result to having unreacted polymerization precursors while with a thick MIP layer, there is a higher tendency for template molecules to be trapped into the polymer matrix, making them harder to be removed. These drawbacks should be taken into consideration when designing a SERS substrate with MIP.

Supplementary Materials: The following are available online at <http://www.mdpi.com/2079-6412/10/8/751/s1>, Figure S1: SERS spectrum of Cypermethrin at a concentration of 10^{-3} M, taken with a 633 nm-wavelength laser. The peaks at 662, 1002, 1165, 1208, 1615, 1740, and 2253 cm^{-1} corresponds to Cypermethrin.

Author Contributions: Investigation and writing, J.S., Y.-C.H., and H.L.; Conceptualization, design, and methodology, Y.C.H., H.-Z.X., H.L., and J.S.; supervision, J.-D.L., W.-E.F., and G.D.C.; review and editing, J.-D.L. and J.S.; funding acquisition, J.-D.L. and H.L. All authors have read and agreed to the published version of the manuscript.

Funding: This research received a grant from Taiwan Ministry of Science and Technology under Grant Nos. 108-2218-E-006-054-MY3 and 108-2811-E-006-535.

Conflicts of Interest: The authors declare no conflict of interest.

References

1. Yuan, Y.; Panwar, N.; Yap, S.H.K.; Wu, Q.; Zeng, S.; Xu, J.; Tjin, S.C.; Song, J.; Qu, J.; Yong, K.T. SERS-based ultrasensitive sensing platform: An insight into design and practical applications. *Coord. Chem. Rev.* **2017**, *337*, 1–33. [CrossRef]
2. Abalde-Cela, S.; Carregal-Romero, S.; Coelho, J.P.; Guerrero-Martínez, A. Recent progress on colloidal metal nanoparticles as signal enhancers in nanosensing. *Adv. Colloid Interface Sci.* **2016**, *233*, 255–270. [CrossRef] [PubMed]
3. Zhang, Y.; Wang, Z.; Wu, L.; Pei, Y.; Chen, P.; Cui, Y. Rapid simultaneous detection of multi-pesticide residues on apple using SERS technique. *Analyst* **2014**, *139*, 5148–5154. [CrossRef] [PubMed]
4. Li, R.; Yang, G.; Yang, J.; Han, J.; Liu, J.; Huang, M. Determination of melamine in milk using surface plasma effect of aggregated Au@SiO₂ nanoparticles by SERS technique. *Food Control* **2016**, *68*, 14–19. [CrossRef]
5. Nawrocka, A.; Lamorska, J. Determination of Food Quality by Using Spectroscopic Methods. In *Advances in Agrophysical Research*; IntechOpen: Rijeka, Croatia, 2013; pp. 347–368.
6. Liu, B.; Zhou, P.; Liu, X.; Sun, X.; Li, H.; Lin, M. Detection of pesticides in fruits by surface-enhanced Raman spectroscopy coupled with gold nanostructures. *Food Bioprocess Technol.* **2013**, *6*, 710–718. [CrossRef]
7. Shan, B.; Pu, Y.; Chen, Y.; Liao, M.; Li, M. Novel SERS labels: Rational design, functional integration and biomedical applications. *Coord. Chem. Rev.* **2018**, *371*, 11–37. [CrossRef]
8. Zito, G.; Rusciano, G.; Sasso, A. Enhancement factor statistics of surface enhanced Raman scattering in multiscale heterostructures of nanoparticles. *J. Chem. Phys.* **2016**, *145*, 054708. [CrossRef]

9. Garcia-leis, A.; Rivera-arreba, I.; Sanchez-cortes, S. Morphological tuning of plasmonic silver nanostars by controlling the nanoparticle growth mechanism: Application in the SERS detection of the amyloid marker Congo Red. *Colloids Surf. A Physicochem. Eng. Asp.* **2017**, *535*, 49–60. [[CrossRef](#)]
10. Joseph, D.; Baskaran, R.; Yang, S.G.; Huh, Y.S.; Han, Y.K. Multifunctional spiky branched gold-silver nanostars with near-infrared and short-wavelength infrared localized surface plasmon resonances. *J. Colloid Interface Sci.* **2019**, *542*, 308–316. [[CrossRef](#)]
11. Park, J.E.; Jung, Y.; Kim, M.; Nam, J.M. Quantitative nanoplasmonics. *ACS Cent. Sci.* **2018**, *4*, 1303–1314. [[CrossRef](#)]
12. Yang, H.; Owiti, E.O.; Jiang, X.; Li, S.; Liu, P.; Sun, X. Localized surface plasmon resonance dependence on misaligned truncated Ag nanoprism dimer. *Nanoscale Res. Lett.* **2017**, *12*, 1–6. [[CrossRef](#)] [[PubMed](#)]
13. Wu, D.; Chen, Y.; Hou, S.; Fang, W.; Duan, H. Intracellular and Cellular Detection by SERS-Active Plasmonic Nanostructures. *ChemBioChem* **2019**, *20*, 2432–2441. [[CrossRef](#)]
14. Sinha, S.S.; Jones, S.; Pramanik, A.; Ray, P.C. Nanoarchitecture Based SERS for Biomolecular Fingerprinting and Label-Free Disease Markers Diagnosis. *Acc. Chem. Res.* **2016**, *49*, 2725–2735. [[CrossRef](#)] [[PubMed](#)]
15. Yoon, H.J.; Kozminsky, M.; Nagrath, S. Emerging role of nanomaterials in circulating tumor cell isolation and analysis. *ACS Nano* **2014**, *8*, 1995–2017. [[CrossRef](#)]
16. Saylan, Y.; Akgönüllü, S.; Yavuz, H.; Ünal, S.; Denizli, A. Molecularly imprinted polymer based sensors for medical applications. *Sensors* **2019**, *19*, 1279. [[CrossRef](#)] [[PubMed](#)]
17. Lingxin, C.; Wang, X.; Lu, W.; Wu, X.; Li, J. Molecular imprinting : Perspectives and applications. *Chem. Soc. Rev.* **2016**, *45*, 2137–2211. [[CrossRef](#)]
18. Li, X.; Yang, T.; Song, Y.; Zhu, J.; Wang, D.; Li, W. Surface-enhanced Raman spectroscopy (SERS)-based immunochromatographic assay (ICA) for the simultaneous detection of two pyrethroid pesticides. *Sens. Actuators B Chem.* **2019**, *283*, 230–238. [[CrossRef](#)]
19. Chao, J.; Cao, W.; Su, S.; Weng, L.; Song, S.; Fan, C.; Wang, L. Nanostructure-based surface-enhanced Raman scattering biosensors for nucleic acids and proteins. *J. Mater. Chem. B* **2016**, *4*, 1757–1769. [[CrossRef](#)]
20. Cowen, T.; Stefanucci, E.; Piletska, E.; Marrazza, G.; Canfarotta, F.; Piletsky, S.A. Synthetic mechanism of molecular imprinting at the solid phase. *Macromolecules* **2020**, *53*, 1435–1442. [[CrossRef](#)]
21. Pekdemir, M.E.; Ertürkan, D.; Külah, H.; Boyacı, İ.H.; Özgen, C.; Tamer, U. Ultrasensitive and selective homogeneous sandwich immunoassay detection by Surface Enhanced Raman Scattering (SERS). *Analyst* **2012**, *137*, 4834–4840. [[CrossRef](#)]
22. Mujahid, A.; Dickert, F.L. Molecularly Imprinted Polymers: Principle, Design, and Enzyme-Like Catalysis. In *Molecularly Imprinted Catalysts*; Elsevier: Amsterdam, The Netherlands, 2016; pp. 79–101. [[CrossRef](#)]
23. Yoshimi, Y.; Sato, K.; Ohshima, M.; Piletska, E. Application of the “gate effect” of a molecularly imprinted polymer grafted on an electrode for the real-time sensing of heparin in blood. *Analyst* **2013**, *138*, 5121–5128. [[CrossRef](#)] [[PubMed](#)]
24. Chen, S.; Dong, L.; Yan, M.; Dai, Z. Rapid and sensitive biomarker detection using molecular imprinting polymer hydrogel and surface-enhanced Raman scattering. *R. Soc. Open Sci* **2018**, *5*, 171488. [[CrossRef](#)] [[PubMed](#)]
25. Wang, F.; Cao, S.; Yan, R.; Wang, Z.; Wang, D.; Yang, H. Selectivity/specificity improvement strategies in surface-enhanced raman spectroscopy analysis. *Sensors* **2017**, *17*, 2689. [[CrossRef](#)] [[PubMed](#)]
26. Wan, L.; Chen, Z.; Huang, C.; Shen, X. Core-shell molecularly imprinted particles. *Trends Anal. Chem.* **2017**, *95*, 110–121. [[CrossRef](#)]
27. Li, Y.; Wang, Y.; Wang, M.; Zhang, J.; Wang, Q.; Li, H. A molecularly imprinted nanoprobe incorporating Cu₂O@Ag nanoparticles with different morphologies for selective SERS based detection of chlorophenols. *Microchim. Acta* **2020**, *187*, 59. [[CrossRef](#)]
28. Holthoff, E.L.; Stratis-Cullum, D.N.; Hankus, M.E. A nanosensor for TNT detection based on molecularly imprinted polymers and surface enhanced Raman scattering. *Sensors* **2011**, *11*, 2700–2714. [[CrossRef](#)]
29. Wang, L.; Xu, Y.; Tan, X.; Tapas, S.; Zhong, J. Aim and shoot : Molecule-imprinting polymer coated MoO₃ for selective SERS detection and photocatalytic destruction of low-level organic contaminants. *RSC Adv.* **2017**, *7*, 36201–36207. [[CrossRef](#)]
30. Arfaoui, F.; Jaoued-grayaa, N.; Riani, A.; Kalfat, R. Synthesis and characterization of molecularly imprinted silica for efficient adsorption of melamine. *J. Tunis. Chem. Soc.* **2017**, *19*, 227–236.

31. Li, H.; Wang, X.; Wang, Z.; Jiang, J.; Qiao, Y.; Wei, M.; Yan, Y.; Li, C. A high-performance SERS-imprinted sensor doped with silver particles of different surface morphologies for selective detection of pyrethroids in rivers. *New J. Chem.* **2017**, *41*, 14342–14350. [[CrossRef](#)]
32. Pohanka, M. Sensors based on molecularly imprinted polymers. *Int. J. Electrochem. Sci.* **2017**, *12*, 8082–8094. [[CrossRef](#)]
33. Guo, X.; Li, J.; Arabi, M.; Wang, X.; Wang, Y.; Chen, L. Molecular-imprinting-based surface-enhanced raman scattering sensors. *ACS Sens.* **2020**, *5*, 601–619. [[CrossRef](#)] [[PubMed](#)]



© 2020 by the authors. Licensee MDPI, Basel, Switzerland. This article is an open access article distributed under the terms and conditions of the Creative Commons Attribution (CC BY) license (<http://creativecommons.org/licenses/by/4.0/>).